

# IUAC School on Nuclear Reactions: The CDCC and CRC methods

**Antonio M. Moro**



Universidad de Sevilla, Spain

**November 15th-20th, 2021**

Material available at: <https://github.com/ammoro/IUAC>



## Course outline I

### 1 The CDCC method

- Reminder of the coupled-channels method
- Single-particle and cluster excitations
- Partial wave analysis: radial equations
- Some examples of applications of the CDCC method
- Exploring the continuum with breakup reactions
- Radiative capture from Coulomb dissociation data

### 2 Advanced CDCC and extensions

- Extension to 3-body projectiles
- Core excitations

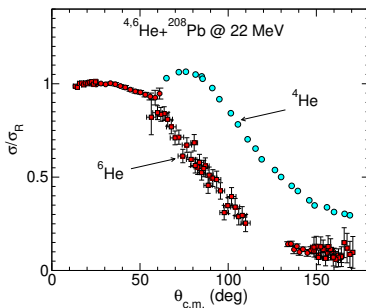
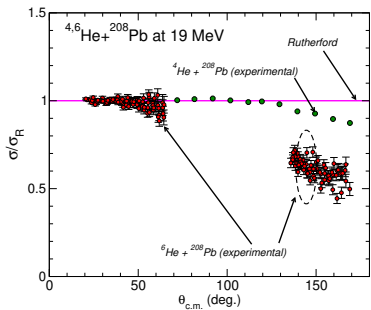
### 3 Application of CDCC to transfer reactions

- Transfer reactions with weakly bound nuclei
- Transfer populating unbound states



## Motivation of the CDCC method

How does the halo structure affect the elastic scattering?



- ⇒ For  $E = 19$  MeV (below the barrier,  $V_b \approx 21$  MeV)  $^4\text{He}$  follows Rutherford formula.
- ⇒  $^6\text{He}$  drastically departs from Rutherford formula at both energies!



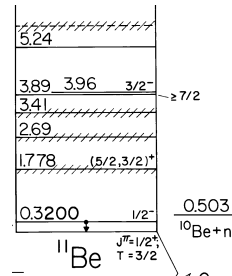
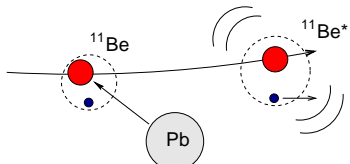


## Reminder of the coupled-channels method



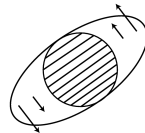
## Inelastic scattering

- ⇒ Nuclei are not inert or *frozen* objects; they do have an internal structure of protons and neutrons that can be modified (excited) during the collision.
- ⇒ Quantum systems exhibit, in general, an energy spectrum with bound and unbound levels.

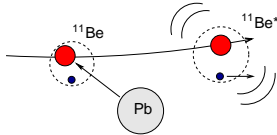


## Models for inelastic excitations

- ① **COLLECTIVE:** Involve a collective motion of several nucleons which can be interpreted macroscopically as **rotations** or **surface vibrations** of the nucleus.



- ② **FEW-BODY/SINGLE-PARTICLE:** Involve the excitation of a nucleon or cluster.





## The coupled-channels method for inelastic scattering

We need to incorporate explicitly in the Hamiltonian the internal structure of the nucleus being excited (e.g. projectile).

$$H = T_R + h(\xi) + V(\mathbf{R}, \xi)$$

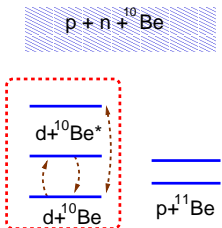
- ⇒  $T_R$ : Kinetic energy for projectile-target relative motion.
- ⇒  $\{\xi\}$ : Internal degrees of freedom of the projectile (depend on the model).
- ⇒  $V(\mathbf{R}, \xi)$ : Projectile-target interaction.
- ⇒  $h(\xi)$ : Internal Hamiltonian of the projectile.

$$h(\xi)\phi_n(\xi) = \varepsilon_n\phi_n(\xi)$$

- ⇒  $\phi_n(\xi)$ : internal states of the projectile.



## Modelscape and scattering wavefunction: $d + {}^{10}\text{Be} \rightarrow d + {}^{10}\text{Be}^*$ example



☞ The modelspace is composed by ground states (elastic channel) and some excited states (inelastic scattering)

Boundary conditions for scattering wavefunction:

$$\Psi_{\mathbf{K}_0}^{(+)}(\mathbf{R}, \xi) \xrightarrow{R \gg} e^{i\mathbf{K}_0 \cdot \mathbf{R}} \phi_0(\xi) + \underbrace{f_{0,0}(\theta)}_{\text{incident}} \frac{e^{iK_0 R}}{R} \phi_0(\xi) + \underbrace{\sum_{n>0} f_{n,0}(\theta)}_{\text{elastic}} \frac{e^{iK_n R}}{R} \phi_n(\xi) + \underbrace{\sum_{n>0} f_{n,0}(\theta)}_{\text{inelastic}} \frac{e^{iK_n R}}{R} \phi_n(\xi)$$

Cross sections:

$$\left( \frac{d\sigma(\theta)}{d\Omega} \right)_{0 \rightarrow n} = \frac{K_n}{K_0} |f_{n,0}(\theta)|^2 \quad f_{n,0}(\theta) = \text{scattering amplitude}$$



## CC model wavefunction (target excitation)

We expand the total wave function in a subset of internal states representing the adopted modelspace:

$$\Psi_{\text{model}}(\mathbf{R}, \xi) = \phi_0(\xi)\chi_0(\mathbf{K}_0, \mathbf{R}) + \sum_{n>0} \phi_n(\xi)\chi_n(\mathbf{K}_n, \mathbf{R})$$

and impose the boundary conditions for the (unknown)  $\chi_n(\mathbf{R})$ :

$$\begin{aligned}\chi_0^{(+)}(\mathbf{K}_0, \mathbf{R}) &\rightarrow e^{i\mathbf{K}_0 \cdot \mathbf{R}} + f_{0,0}(\theta) \frac{e^{iK_0 R}}{R} && \text{for } n=0 \text{ (elastic)} \\ \chi_n^{(+)}(\mathbf{K}_n, \mathbf{R}) &\rightarrow f_{n,0}(\theta) \frac{e^{iK_n R}}{R} && \text{for } n>0 \text{ (non-elastic)}\end{aligned}$$



## Calculation of $\chi_n^{(+)}(\mathbf{R})$ : the coupled equations

- ⇒ The model wavefunction must satisfy the Schrödinger equation:

$$[H - E]\Psi_{\text{model}}^{(+)}(\mathbf{R}, \xi) = 0$$

- ⇒ Multiply on the left by each  $\phi_n^*(\xi)$ , and integrate over  $\xi \Rightarrow$  coupled channels equations for  $\{\chi_n(\mathbf{R})\}$ :

$$[E - \varepsilon_n - T_R - V_{n,n}(\mathbf{R})]\chi_n(\mathbf{R}) = \sum_{n' \neq n} V_{n,n'}(\mathbf{R})\chi_{n'}(\mathbf{R})$$

- ⇒ The structure information is embedded in the coupling potentials:

$$V_{n,n'}(\mathbf{R}) = \int d\xi \phi_{n'}^*(\xi) V(\mathbf{R}, \xi) \phi_n(\xi)$$

☞  $\phi_n(\xi)$  will depend on the assumed structure model (collective, few-body, etc).



## Optical Model vs. Coupled-Channels method

### Optical Model

⇒ The Hamiltonian:

$$H = T_R + V(\mathbf{R})$$

⇒ Internal states: Just  $\phi_0(\xi)$

⇒ Model wavefunction:

$$\Psi_{\text{mod}}(\mathbf{R}, \xi) \equiv \chi_0(\mathbf{K}, \mathbf{R}) \phi_0(\xi)$$

⇒ Schrödinger equation:

$$[H - E]\chi_0(\mathbf{K}, \mathbf{R}) = 0$$



## Optical Model vs. Coupled-Channels method

### Optical Model

⇒ The Hamiltonian:

$$H = T_R + V(\mathbf{R})$$

⇒ Internal states: Just  $\phi_0(\xi)$

⇒ Model wavefunction:

$$\Psi_{\text{mod}}(\mathbf{R}, \xi) \equiv \chi_0(\mathbf{K}, \mathbf{R})\phi_0(\xi)$$

⇒ Schrödinger equation:

$$[H - E]\chi_0(\mathbf{K}, \mathbf{R}) = 0$$

### Coupled-channels method

⇒ The Hamiltonian:

$$H = T_R + h(\xi) + V(\mathbf{R}, \xi)$$

⇒ Internal states:

$$h(\xi)\phi_n(\xi) = \varepsilon_n\phi_n(\xi)$$

⇒ Model wavefunction:

$$\Psi_{\text{model}}(\mathbf{R}, \xi) = \phi_0(\xi)\chi_0(\mathbf{K}, \mathbf{R}) + \sum_{n>0} \phi_n(\xi)\chi_n(\mathbf{K}, \mathbf{R})$$

⇒ Schrödinger equation:

$$[H - E]\Psi_{\text{model}}(\mathbf{R}, \xi) = 0$$



$$[E - \varepsilon_n - T_R - V_{n,n}(\mathbf{R})]\chi_n(\mathbf{K}, \mathbf{R}) = \sum_{n' \neq n} V_{n,n'}(\mathbf{R})\chi_{n'}(\mathbf{K}, \mathbf{R})$$



## DWBA approximation as 1st order CC

⇒ Two-states model  $n = 0, 1$ :

$$\Psi(\mathbf{R}, \xi) = \underbrace{\phi_0(\xi)\chi_0(\mathbf{R})}_{\text{elastic}} + \underbrace{\phi_1(\xi)\chi_1(\mathbf{R})}_{\text{inelastic}}$$

⇒ Coupled-channels equations:

$$[E - \varepsilon_0 - T_0 - V_{00}(\mathbf{R})]\chi_0(\mathbf{R}) = V_{01}(\mathbf{R})\chi_1(\mathbf{R})$$

$$[E - \varepsilon_1 - T_1 - V_{11}(\mathbf{R})]\chi_1(\mathbf{R}) = V_{10}(\mathbf{R})\chi_0(\mathbf{R})$$

⇒ Iterative solution of the CC equations (DWBA):

$$[E - \varepsilon_0 - T_0 - V_{00}(\mathbf{R})]\chi_0(\mathbf{R}) \approx 0$$

$$[E - \varepsilon_1 - T_1 - V_{11}(\mathbf{R})]\chi_1(\mathbf{R}) \approx V_{10}(\mathbf{R})\chi_0(\mathbf{R})$$

## DWBA approximation as 1st order CC

⇒ Asymptotically:

$$\chi_1^{(+)}(\mathbf{R}) \rightarrow f_{10}(\theta) \frac{e^{iK_1 R}}{R}$$

with (not proven here!)

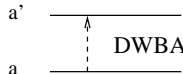
$$f_{10}(\theta) = -\frac{2\mu}{4\pi\hbar^2} \int d\mathbf{R} \tilde{\chi}_1^{(-)*}(\mathbf{K}_1, \mathbf{R}) V_{10}(\mathbf{R}) \tilde{\chi}_0^{(+)}(\mathbf{K}_0, \mathbf{R})$$

where  $\tilde{\chi}_0(\mathbf{K}_0, \mathbf{R}), \tilde{\chi}_1(\mathbf{K}_1, \mathbf{R})$  are solutions of:

$$[E - \varepsilon_0 - T_0 - V_{00}(\mathbf{R})] \tilde{\chi}_0(\mathbf{K}_0, \mathbf{R}) = 0$$

$$[E - \varepsilon_1 - T_1 - V_{11}(\mathbf{R})] \tilde{\chi}_1(\mathbf{K}_1, \mathbf{R}) = 0$$

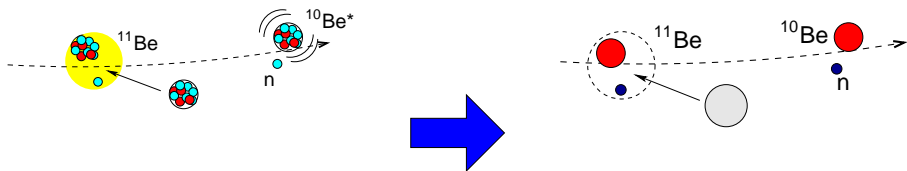
⇒ The DWBA approximation amounts at solving the CC equations to 1st order (Born approximation)



## Single-particle and cluster excitations



## Many-body to few-body reduction



$$\mathcal{V}_{pt} = \sum_{ij} V_{ij}(\mathbf{r}_{ij})$$

$$\mathcal{V}_{pt} = U_{ct}(\mathbf{r}_{ct}) + U_{nt}(\mathbf{r}_{nt})$$

⇒ Effective **three-body** Hamiltonian:

$$H = T_{\mathbf{R}} + h_r(\mathbf{r}) + U_{ct}(\mathbf{r}_{ct}) + U_{nt}(\mathbf{r}_{nt})$$

⇒  $U_{ct}(\mathbf{r}_{ct}), U_{nt}(\mathbf{r}_{nt})$  are optical potentials describing fragment-target elastic scattering (eg. target excitation is treated effectively, through absorption)

## Inelastic scattering in a few-body model

- Some nuclei allow a description in terms of two or more clusters:  
 $d = p + n$ ,  ${}^6\text{Li} = \alpha + d$ ,  ${}^7\text{Li} = \alpha + {}^3\text{H}$ .
- Projectile-target interaction:

$$V(\mathbf{R}, \xi) \equiv V(\mathbf{R}, \mathbf{r}) = U_1(\mathbf{r}_1) + U_2(\mathbf{r}_2)$$

- Transition potentials:

$$V_{n,n'}(\mathbf{R}) = \int d\mathbf{r} \phi_n^*(\mathbf{r}) [U_1(\mathbf{r}_1) + U_2(\mathbf{r}_2)] \phi_{n'}(\mathbf{r})$$



## Inelastic scattering in a few-body model

- ⇒ Some nuclei allow a description in terms of two or more clusters:  
 $d=p+n$ ,  ${}^6\text{Li}=\alpha+d$ ,  ${}^7\text{Li}=\alpha+{}^3\text{H}$ .
- ⇒ Projectile-target interaction:

$$V(\mathbf{R}, \xi) \equiv V(\mathbf{R}, \mathbf{r}) = U_1(\mathbf{r}_1) + U_2(\mathbf{r}_2)$$

- ⇒ Transition potentials:

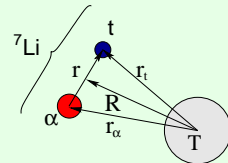
$$V_{n,n'}(\mathbf{R}) = \int d\mathbf{r} \phi_n^*(\mathbf{r}) [U_1(\mathbf{r}_1) + U_2(\mathbf{r}_2)] \phi_{n'}(\mathbf{r})$$

**Example:**  ${}^7\text{Li}=\alpha+t$

$$\mathbf{r}_\alpha = \mathbf{R} - \frac{m_t}{m_\alpha + m_t} \mathbf{r}; \quad \mathbf{r}_t = \mathbf{R} + \frac{m_\alpha}{m_\alpha + m_t} \mathbf{r}$$

**Internal states:** (two-body cluster model)

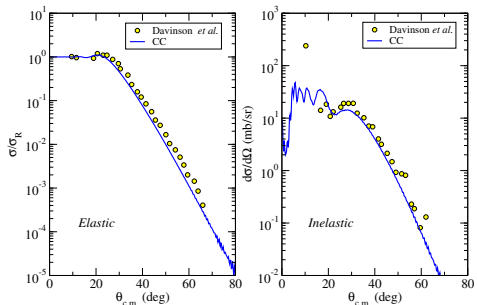
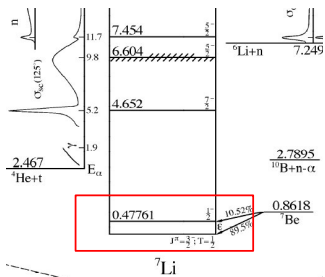
$$[T_{\mathbf{r}} + V_{\alpha-t}(\mathbf{r}) - \varepsilon_n] \phi_n(\mathbf{r}) = 0$$





## Example: ${}^7\text{Li}(\alpha+t) + {}^{208}\text{Pb}$ at 68 MeV

⇒ CC calculation with 2 channels ( $3/2^-$ ,  $1/2^-$ ):



Data from Davinson et al, Phys. Lett. 139B (1984) 150

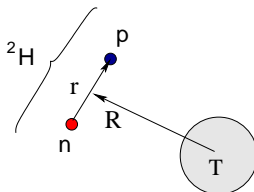
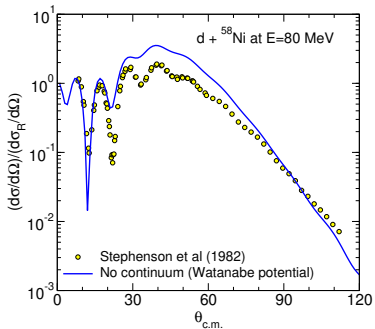
Fresco input available at <https://github.com/ammoro/IUAC>



## Application of the CC method to weakly-bound systems

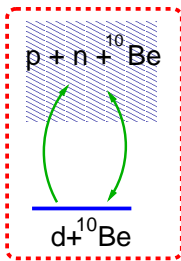
**Example:** Three-body calculation ( $p + n + {}^{58}\text{Ni}$ ) with Watanabe potential:

$$V_{dt}(\mathbf{R}) = \int d\mathbf{r} \phi_{gs}^*(\mathbf{r}) \left\{ V_{pt}(\mathbf{r}_{pt}) + V_{nt}(\mathbf{r}_{nt}) \right\} \phi_{gs}(\mathbf{r})$$



☞ Three-body calculations omitting breakup channels fail to describe the experimental data.

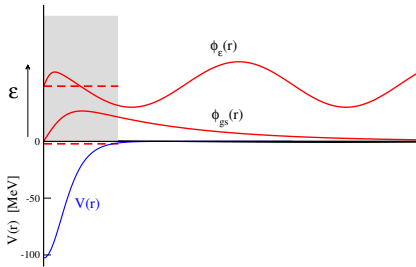
## Extension of the CC to unbound states



We want to include explicitly in the modelspace the breakup channels of the projectile or target.



## Bound versus scattering states

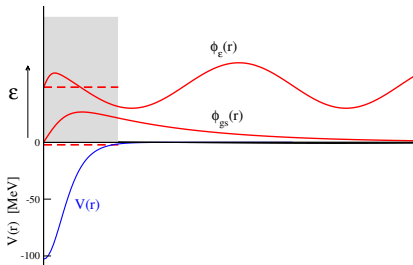


Continuum wavefunctions:

$$\varphi_{k,\ell jm}(\mathbf{r}) = \frac{u_{k,\ell j}(r)}{r} [Y_\ell(\hat{r}) \otimes \chi_s]_{jm}$$

$$\epsilon = \frac{\hbar^2 k^2}{2\mu}$$

## Bound versus scattering states



Continuum wavefunctions:

$$\varphi_{k,\ell jm}(\mathbf{r}) = \frac{u_{k,\ell j}(r)}{r} [Y_\ell(\hat{r}) \otimes \chi_s]_{jm}$$

$$\varepsilon = \frac{\hbar^2 k^2}{2\mu}$$

Unbound states are not suitable for CC calculations:

- ⇒ They have a continuous (infinite) distribution in energy.
- ⇒ Non-normalizable:  $\langle u_{k,\ell sj}(r) | u_{k',\ell sj}(r) \rangle \propto \delta(k - k')$

**SOLUTION ⇒ continuum discretization**



# The origins of CDCC

- ⇒ Continuum discretization method proposed by G.H. Rawitscher [PRC9, 2210 (1974)] and Farrell, Vincent and Austern [Ann.Phys.(New York) 96, 333 (1976)] to describe deuteron scattering as an effective three-body problem  $p + n + A$ .

PHYSICAL REVIEW C

VOLUME 9, NUMBER 6

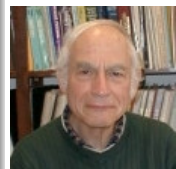
JUNE 1974

## Effect of deuteron breakup on elastic deuteron-nucleus scattering

George H. Rawitscher\*

*Center for Theoretical Physics, Massachusetts Institute of Technology, Cambridge, Massachusetts 02139,  
and Department of Physics, University of Surrey, Guildford, Surrey, England  
(Received 1 October 1973; revised manuscript received 4 March 1974)*

The properties of the transition matrix elements  $V_{ab}(R)$  of the breakup potential  $V_N$  taken between states  $\phi_a(\vec{r})$  and  $\phi_b(r)$  are examined. Here  $\phi_a(\vec{r})$  are eigenstates of the neutron-proton relative-motion Hamiltonian, and the eigenvalues of the energy  $\epsilon_a$  are positive (continuum states) or negative (bound deuteron);  $V_N(\vec{r}, \vec{R})$  is the sum of the phenomenological proton-nucleus  $V_{p-A}(|\vec{R} - \frac{1}{2}\vec{r}|)$  and neutron nucleus  $V_{n-A}(|\vec{R} + \frac{1}{2}\vec{r}|)$  optical potentials evaluated for nucleon energies equal to half the incident deuteron energy. The bound-to-continuum transition matrix element for relative neutron-proton angular momenta  $l=2$  are found to be comparable in magnitude to the ones for  $l=0$  for values of  $\epsilon_a$  larger than about 3 MeV, and both decrease only slowly with  $\epsilon_a$ , suggesting that a large breakup spectrum is involved in deuteron-nucleus collisions. The effect of the various breakup transitions on the elastic phase shifts is estimated by numerically solving a set of coupled equations. These equations couple the functions  $\chi_a(\vec{R})$  which are the coefficients of the expansion of the neutron-proton-nucleus wave function in a set of the  $\phi_b(\vec{r})$ 's. The equations are rendered manageable by performing a (rather crude) discretization in the neutron-proton relative-momentum variable  $k_a$ . Numer-

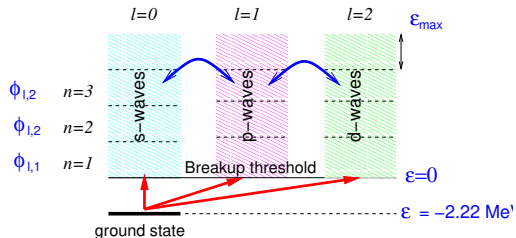


George Rawitscher  
(1928-2018)

- ⇒ Full numerical implementation by Kyushu group (Sakuragi, Yahiro, Kamimura, and co.): Prog. Theor. Phys.(Kyoto) 68, 322 (1982)



## Continuum discretization for deuteron scattering



- ⇒ Select a number of angular momenta ( $\ell = 0, \dots, \ell_{\max}$ ).
- ⇒ For each  $\ell$ , set a maximum excitation energy  $\varepsilon_{\max}$ .
- ⇒ Divide the interval  $\varepsilon = 0 - \varepsilon_{\max}$  in a set of sub-intervals (*bins*).
- ⇒ For each *bin*, calculate a representative wavefunction.

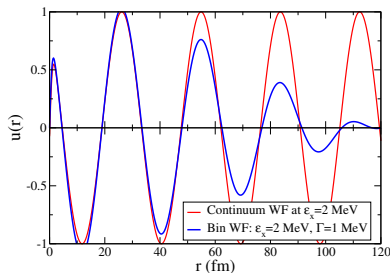
## CDCC formalism: construction of the bin wavefunctions

### Bin wavefunction:

$$\phi_{\ell jm}^{[k_1, k_2]}(\mathbf{r}) = \frac{u_{\ell j}^{[k_1, k_2]}(r)}{r} [Y_\ell(\hat{r}) \otimes \chi_s]_{jm} \quad [k_1, k_2] = \text{bin interval}$$

$$u_{\ell sjm}^{[k_1, k_2]}(r) = \sqrt{\frac{2}{\pi N}} \int_{k_1}^{k_2} w(k) u_{k, \ell sj}(r) dk$$

- ⇒  $k$ : linear momentum
- ⇒  $u_{k, \ell sj}(r)$ : scattering states (radial part)
- ⇒  $w(k)$ : weight function



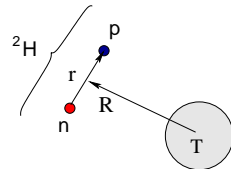


## CDCC formalism for deuteron scattering

- ⇒ Hamiltonian:  $H = T_{\mathbf{R}} + h_r(\mathbf{r}) + V_{pt}(\mathbf{r}_{pt}) + V_{nt}(\mathbf{r}_{nt})$
- ⇒ Model wavefunction:

$$\Psi^{(+)}(\mathbf{R}, \mathbf{r}) = \phi_{gs}(\mathbf{r})\chi_0(\mathbf{R}) + \sum_{n>0}^N \phi_n(\mathbf{r})\chi_n(\mathbf{R})$$

- ⇒ Coupled equations:  $[H - E]\Psi(\mathbf{R}, \mathbf{r}) = 0$



$$[E - \varepsilon_n - T_R - V_{n,n}(\mathbf{R})]\chi_n(\mathbf{R}) = \sum_{n' \neq n} V_{n,n'}(\mathbf{R})\chi_{n'}(\mathbf{R})$$

- ⇒ Transition potentials:

$$V_{n;n'}(\mathbf{R}) = \int d\mathbf{r} \phi_n^*(\mathbf{r}) \left[ V_{pt}(\mathbf{R} + \frac{\mathbf{r}}{2}) + V_{nt}(\mathbf{R} - \frac{\mathbf{r}}{2}) \right] \phi_{n'}(\mathbf{r})$$

## Partial-wave decomposition of CDCC wavefunction

- ⇒ In practical calculations, the CDCC wf is expanded in the so-called **channel basis**

$$\langle \hat{R}, \mathbf{r}, |\beta; J_T \rangle = [Y_L(\hat{R}) \otimes \phi_{n, J_p}(\mathbf{r})]_{J_T} :$$

$$\Psi_{\beta_0, J_T, M_T}(\vec{R}, \vec{r}, \xi) = \sum_{\beta} \frac{\chi_{\beta, \beta_0}^{J_T}(R)}{R} |\beta; J_T \rangle \quad \beta \equiv \{L, J_p, n\}$$

- ⇒ The radial coefficients verify

$$\left( -\frac{\hbar^2}{2\mu} \frac{d^2}{dR^2} + \frac{\hbar^2 L(L+1)}{2\mu R^2} + \varepsilon_n - E \right) \chi_{\beta, \beta_0}^{J_T}(R) + \sum_{\beta'} V_{\beta, \beta'}^{J_T}(R) \chi_{\beta'}^{J_T}(R) = 0$$

with the coupling potentials:

$$V_{\beta, \beta'}^{J_T}(R) = \langle \beta; J_T | V_1(\vec{R}, \vec{r}) + V_2(\vec{R}, \vec{r}) | \beta'; J_T \rangle$$

- ⇒ Boundary conditions:

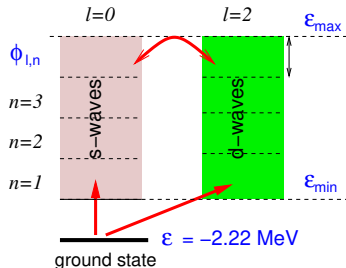
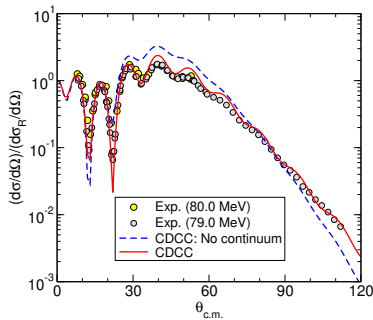
$$\chi_{\beta, \beta_0}^{J_T}(R) \rightarrow e^{i\sigma_L} \frac{i}{2} \left[ H_L^{(-)}(K_{\beta} R) \delta_{\beta_0, \beta} - S_{\beta, \beta_0}^{J_T} H_L^{(+)}(K_{\beta} R) \right]$$



## Applications of the CDCC formalism: d+ $^{58}\text{Ni}$

Coupling to continuum states produce:

- ⇒ Polarization of the projectile (modification of real part)
- ⇒ Flux removal (absorption) from the elastic channel (imaginary part)





## Two- and three-body breakup observables

- CDCC scattering amplitudes readily provide **two-body breakup** observables:

$$\frac{d\sigma_n}{d\Omega_{\text{c.m.}}} = |f_{0,n}(\theta)|^2 \Rightarrow \frac{d^2\sigma}{d\Omega_{\text{c.m.}} d\epsilon_{pn}} \simeq \frac{1}{\Delta_n} \frac{d\sigma_n}{d\Omega_{\text{c.m.}}}$$

with:

- $\Delta_n$ =width of the bin containing the relative energy  $\epsilon_{pn}$
- $\Omega_{\text{c.m.}}$ =C.M. scattering angle of the projectile c.m. (not easy to measure!)

- Three-body observables** can be also calculated using a suitable combination of the scattering amplitudes and appropriate kinematical transformations ([Tostevin, PRC63, 024617 \(2001\)](#)):

$$\frac{d^3\sigma}{d\Omega_n d\Omega_p dE_p}$$

- N.b.:** These 3-body observables are not directly provided by FRESCO. They must be computed separately from the calculated amplitudes.

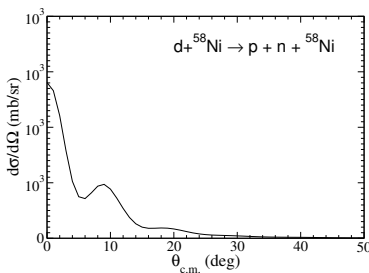


## Two-body breakup observables: $d + {}^{58}\text{Ni} \rightarrow p + n + {}^{58}\text{Ni}$

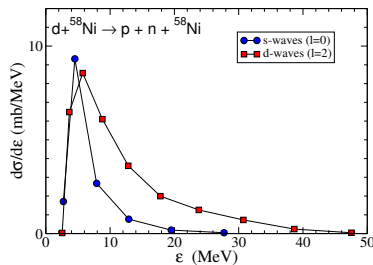
### CDCC calculations for $d + {}^{58}\text{Ni}$ at 80 MeV :

- ⇒ Continuum states with  $\ell = 0, 2$ .
- ⇒ Proton and neutron intrinsic spins ignored.
- ⇒  $p/n + {}^{58}\text{Ni}$  from global optical potential.
- ⇒  $p+n$  simple Gaussian interaction describing deuteron g.s.

$p + n$  c.m. angular distribution



Excitation energy distribution



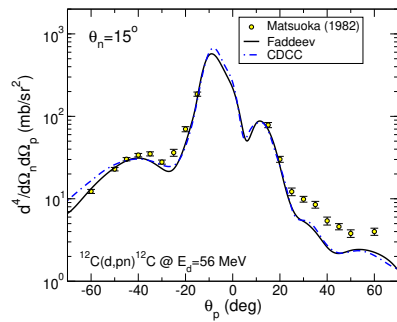
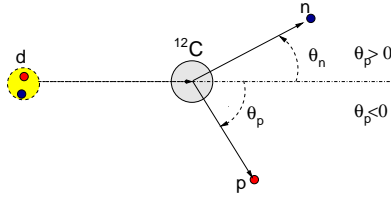


## Breakup observables with CDCC: exclusive breakup of $d + {}^{12}\text{C} \rightarrow p + n + {}^{12}\text{C}$

### CDCC calculations for $d + {}^{12}\text{C}$ at 56 MeV:

- ⇒ Continuum states with  $\ell \leq 8$  and  $\varepsilon_{\max} = 46$  MeV.
- ⇒ Proton and neutron intrinsic spins ignored
- ⇒  $p/n + {}^{58}\text{Ni}$  from Watson global optical potential
- ⇒  $p+n$  simple Gaussian interaction describing deuteron g.s.

**Data:** Matsuoka *et al.*, NPA391, 357 (1986).



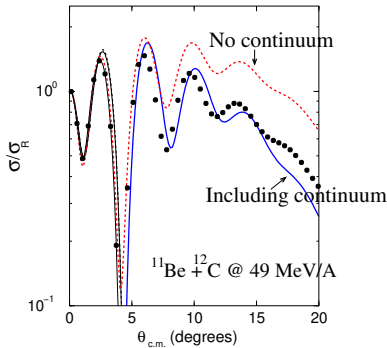
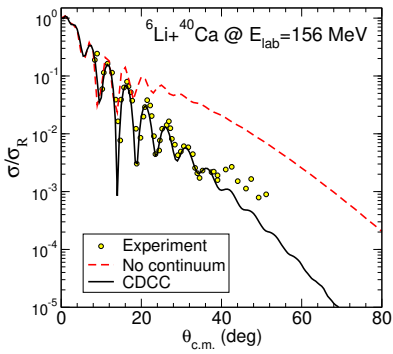
A.Deltuva, A.M.M., E.Cravo, F.M.Nunes, A.C.Fonseca, PRC 76, 064602 (2007)



## Application of the CDCC method to other weakly bound two-body nuclei

The CDCC has been also applied to nuclei with a cluster structure:

- ⇒  $^6\text{Li} = \alpha + \text{d}$  ( $S_{\alpha,\text{d}} = 1.47 \text{ MeV}$ )
- ⇒  $^{11}\text{Be} = ^{10}\text{Be} + \text{n}$  ( $S_n = 0.504 \text{ MeV}$ )

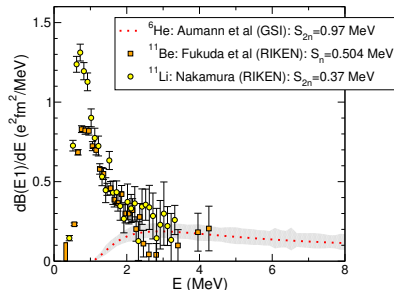
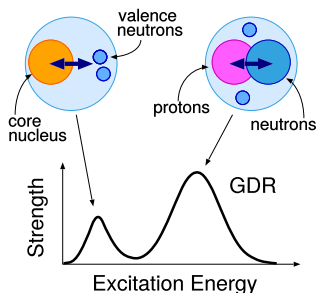




## Exploring the continuum with breakup reactions



## Electric response of weakly-bound nuclei



- ⇒ The  $E\lambda$  response can be quantified through the  $B(E\lambda)$  probability:

$$B(E\lambda; i \rightarrow f) = \frac{1}{2I_i + 1} |\langle \Psi_f | \mathcal{M}(E\lambda) | \Psi_i \rangle|^2$$

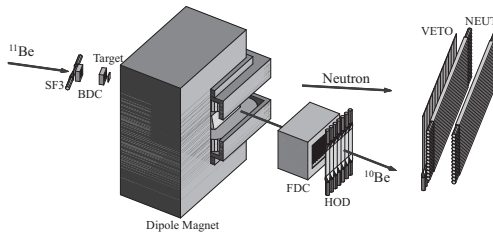
- ⇒ Neutron-halo nuclei have large  $B(E1)$  strengths near threshold



## How to probe/extract the $B(E1)$ of halo nuclei?

**Example:**  $^{11}\text{Be} + ^{208}\text{Pb} \rightarrow ^{10}\text{Be} + \text{n} + ^{208}\text{Pb}$  measured at RIKEN (69 MeV/u).

Fukuda et al, PRC70, 054606 (2004))



- 11Be excitation energy can be reconstructed from core-neutron coincidences (*invariant mass method*)

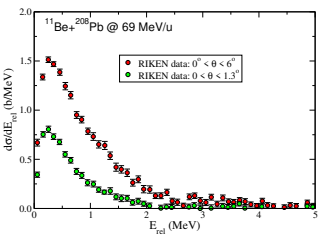
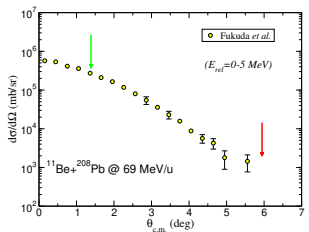


## What observables are measured in Coulomb dissociation experiments?

- ⇒ In a fully exclusive experiment, one can in principle measure the angular and relative energy distribution of the  $^{11}\text{Be}^*$  system:

$$\frac{d^2\sigma}{d\Omega dE_{\text{rel}}}$$

- ⇒ Integrating over the angle or energy, single differential cross sections are obtained:



- ⇒ In the Coulomb dominated region (i.e. small angles), the **breakup cross section** is expected to be dominated by the  $dB(E\lambda)/dE$  distribution, but we need a theory that relates both observables.



## Semiclassical 1st order E $\lambda$ excitation (Alder & Winther) (akin EPM method)

- For E $\lambda$  excitation to bound states ( $0 \rightarrow n$ ):

$$\left( \frac{d\sigma}{d\Omega} \right)_{0 \rightarrow n} = \left( \frac{Z_t e^2}{\hbar v} \right)^2 \frac{B(E\lambda, 0 \rightarrow n)}{e^2 a_0^{2\lambda-2}} f_\lambda(\theta, \xi)$$

$$\xi_{0 \rightarrow n} = \frac{(E_n - E_0)}{\hbar} \frac{a_0}{v}$$

- For continuum states (breakup):

$$\frac{d\sigma(E\lambda)}{d\Omega dE} = \left( \frac{Z_t e^2}{\hbar v} \right)^2 \frac{1}{e^2 a_0^{2\lambda-2}} \frac{dB(E\lambda)}{dE} \frac{df_\lambda(\theta, \xi)}{d\Omega}$$

- $dB(E\lambda)/dE$  can be extracted from small-angle Coulomb dissociation data.

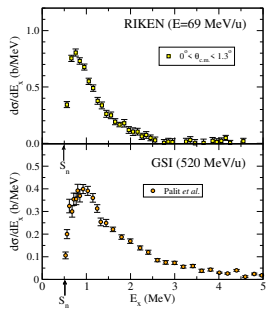
$$\frac{d\sigma}{dE}(\theta < \theta_{\max}) = \int_0^{\theta_{\max}} \frac{d\sigma(E\lambda)}{d\Omega dE} d\Omega \propto \frac{dB(E\lambda)}{dE}$$



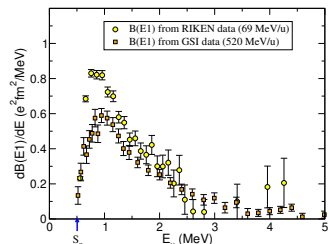
## Extracting $B(E1)$ of $^{11}\text{Be}$ from $^{11}\text{Be} + ^{208}\text{Pb}$ Coulomb dissociation

Common assumptions:

- ⇒ Breakup dominated by Coulomb excitation
- ⇒ Nuclear excitation, if present, can be estimated and added incoherently
- ⇒ If the assumptions above are fulfilled, the extracted  $dB(E\lambda)/dE$  should be independent of the incident energy and target employed, since it reflects a structure property of the projectile.



$$\frac{dB(E\lambda)}{dE} \propto \frac{d\sigma}{dE}$$



RIKEN: Fukuda et al, PRC70 (2004) 054606  
GSI: Palit et al, PRC68 (2003) 034318

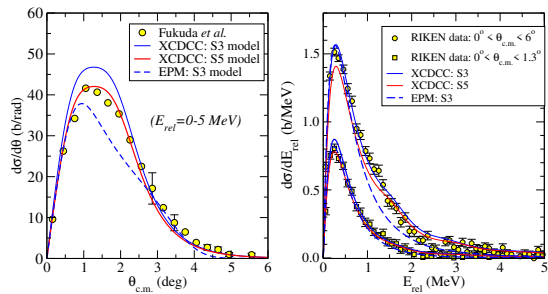
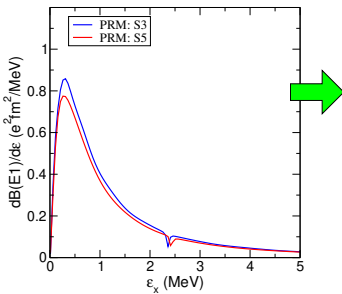
- ⇒ The extracted  $dB(E\lambda)/dE$  distributions are reasonably compatible, but with apparent differences at the peak



## CDCC analysis of Coulomb dissociation data

- ⇒ Nuclear excitation not negligible, even for small  $\theta$
- ⇒ Nuclear contribution interferes with Coulomb
- ⇒ Higher-order couplings can affect the cross sections
- ⇒ These ingredients can be naturally incorporated within the CDCC method (at the expense of more complexity!)

E.g.: CDCC analysis based on two-body  $^{10}\text{Be} + \text{n}$  model:



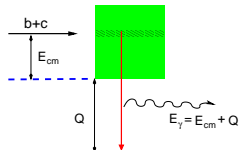
- ⇒ Different structure models yield different  $B(E1)$  strengths and hence different breakup cross sections
- ⇒ Comparison with the angular distribution evidences the deficiencies of the semiclassical EPM model

PLB 811 (2020) 135959

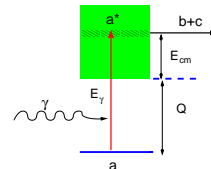


## Application to radiative capture reactions

Radiative capture:  $b + c \rightarrow a + \gamma$



Photodissociation:  $a + \gamma \rightarrow b + c$



⇒ Related by detailed balance:

$$\sigma_{E\lambda}^{(rc)} = \frac{2(2J_a + 1)}{(2J_b + 1)(2J_c + 1)} \frac{k_\gamma^2}{k^2} \sigma_{E\lambda}^{(phot)} \quad (\hbar k_\gamma = E_\gamma/c)$$

⇒ Astrophysical S-factor:

$$S(E_{c.m.}) = E_{c.m.} \sigma_{E\lambda}^{(rc)} \exp[2\pi\eta(E_{c.m.})]$$

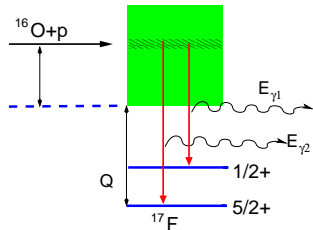
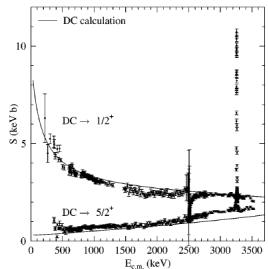
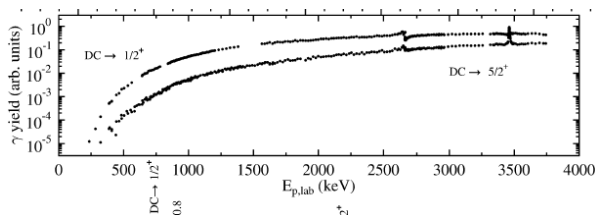
⇒ Capture cross sections are difficult to measure because they are very small at relevant astrophysical energies.



## Direct determination of radiative capture cross sections

**Example:**  $p + ^{16}\text{O} \rightarrow ^{17}\text{F} + \gamma$

Morlock, PRL79, 3837 (1997)





## Indirect determination of radiative capture from Coulomb breakup

⇒ The photodissociation ( $\gamma + a \rightarrow b + c$ ) cross section is related to the  $B(E\lambda)$

$$\sigma_{E\lambda}^{\text{photo}} = \frac{(2\pi)^3(\lambda + 1)}{\lambda[(2\lambda + 1)!!]^2} \left( \frac{E_\gamma}{\hbar c} \right)^{2\lambda-1} \frac{dB(E\lambda)}{dE}$$

⇒ Then, in 1st order semiclassical limit, the Coulomb breakup x-section is proportional to photodissociation x-section:

$$\boxed{\frac{d\sigma(E\lambda)}{d\Omega dE_\gamma} = \frac{1}{E_\gamma} \frac{dn_{E\lambda}}{d\Omega} \sigma_{E\lambda}^{\text{photo}}} \quad (\text{Equivalent Photon Method})$$

with the virtual photon number

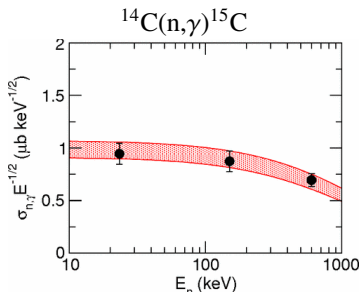
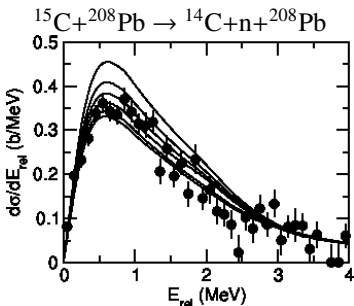
$$\frac{dn_{E\lambda}}{d\Omega} = Z_t^2 \alpha \frac{\lambda[(2\lambda + 1)!!]^2}{(2\pi)^3(\lambda + 1)} \xi^{2(1-\lambda)} \left( \frac{c}{v} \right)^{2\lambda} \frac{df_{E\lambda}}{d\Omega}$$



## Radiative capture from Coulomb dissociation experiments

- Capture reactions have typically small cross sections
- As an alternative, one can indirectly obtain the capture cross sections from Coulomb dissociation experiments involving the same two-body projectile:

$$\frac{d\sigma}{d\Omega dE_{c.m.}} \rightarrow \sigma_{E\lambda}^{(\text{phot})} \rightarrow \sigma_{E\lambda}^{(rc)} \rightarrow S(E_{c.m.})$$

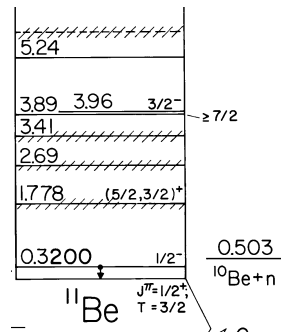


(dots: direct; shaded region: from Coulomb breakup)  
Summers and Nunes, PRC 78, 011601(R), 2008



## Exploring structures in the continuum

The continuum spectrum is not “homogeneous”; it contains in general energy regions with special structures, such as resonances and virtual states



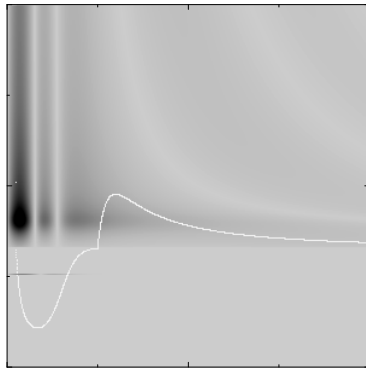


## What is a resonance?

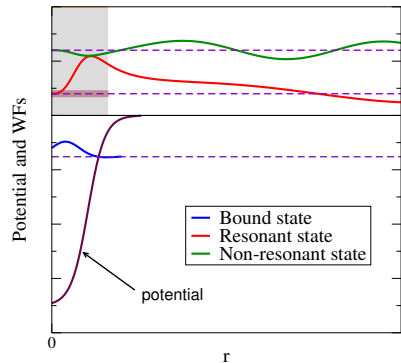
- ⇒ It is a **pole** of the S-matrix in the complex energy plane.
- ⇒ It is a structure on the continuum which may, or may not, produce a **maximum in the cross section**, depending on the reaction mechanism and the phase space available.
- ⇒ The resonance occurs in the range of energies for which the **phase shift is close to  $\pi/2$** .
- ⇒ In this range of energies, **the continuum wavefunctions is largely localized** within the radial range of the potential.
- ⇒ The continuum wavefunctions are **not square normalizable**. For practical reasons, a normalized wave-packet (or “bin”) can be constructed to represent the resonance.

## Distinctive features of a resonance

In the energy range of the resonance, the continuum wavefunctions have a large probability of being within the range of the potential.

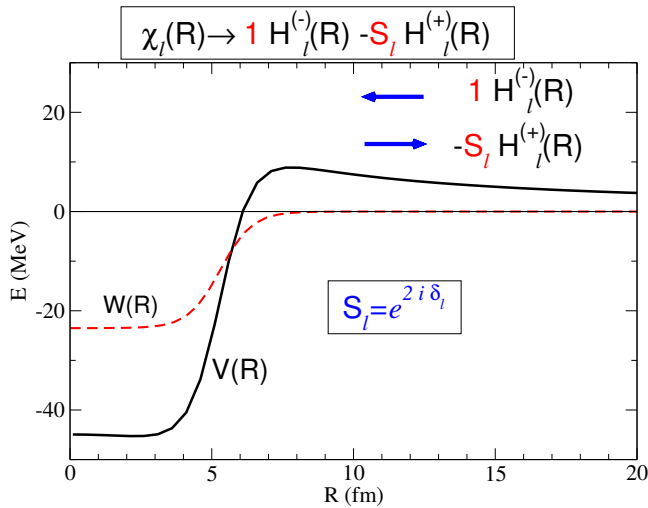


(Courtesy of C. Dasso)



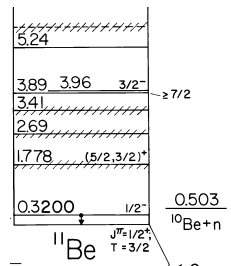
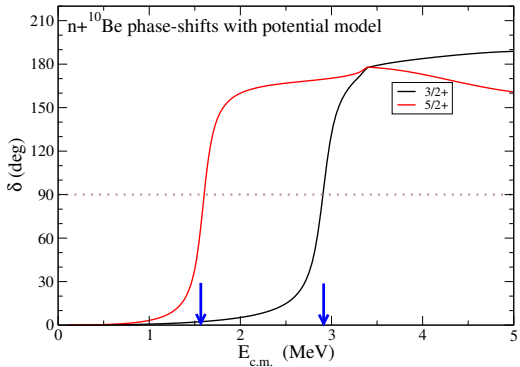


## Resonances and phase-shifts





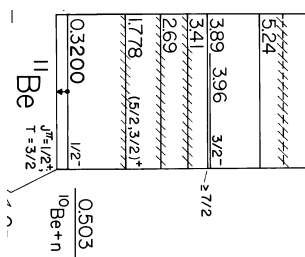
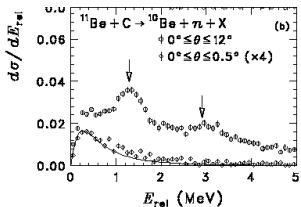
## Resonances and phase-shifts



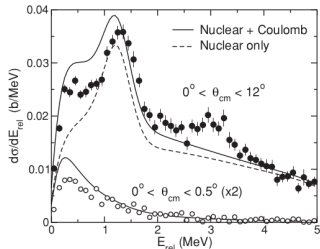
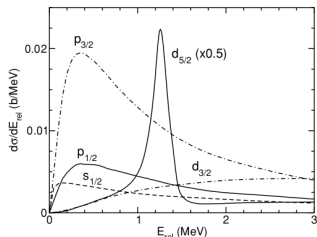


# Studying resonances in nuclear breakup experiments

RIKEN data



CDCC analysis





## Proposed exercise

Consider a simple two-body model for a one-neutron halo nucleus. For E1 transitions, the electric transition probability is given by

$$\frac{dB(E1)}{dE_c} = \left( \frac{4\pi}{k} \right)^2 \frac{\mu k}{(2\pi)^3 \hbar^2} \frac{3}{4\pi} \left( \frac{Ze}{A} \right)^2 \left| \langle \ell_i 010 | \ell_f 0 \rangle \int dr r^2 \phi_f(k, r) \phi_i(r) \right|^2$$

where  $\mu$  is the reduced mass of the two-body system,  $\phi_i(r)$  is the radial part of the ground-state wavefunction and  $\phi_f(k, r)$  is the radial part of the positive-energy state with energy  $E_c = \hbar^2 k^2 / 2\mu$  and asymptotic behaviour  $\phi_f(k, r) \xrightarrow{r \gg} (kr) j_\ell(kr)$

- ⇒ Show that, in the special case in which the final states are approximated by plane waves, the  $B(E1)$  distribution is related to the Fourier transform of the ground state wavefunction. Give arguments to justify that, in the case of weakly bound systems, the  $B(E1)$  distribution is concentrated at low excitation energies.



## Exercises

- ⇒ In the situation above, the ground state wavefunction can be approximated by its asymptotic form which, for a  $s$ -wave configuration, can be written as

$$\phi_i(r) \simeq \sqrt{2k_0} e^{-k_0 r} / r.$$

Give the expression for  $k_0$  in terms of the neutron separation energy ( $S_n$ ) and the reduced mass of the neutron-core system. Compute it numerically for the  $^{11}\text{Be}$  ( $^{10}\text{Be} + n$ ) case.

- ⇒ Show that, under these approximations, the  $B(E1)$  distribution is given by

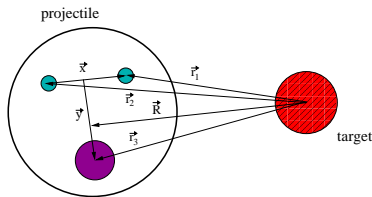
$$\frac{dB(E1)}{dE_c} = \frac{3\hbar^2}{\pi^2 \mu} \left(\frac{Ze}{A}\right)^2 \frac{\sqrt{S_n} E_c^{3/2}}{(E_c + S_n)^4}.$$

**Hint:**  $\int_0^\infty dr r^2 j_1(br) e^{-ar} = 2b/(a^2 + b^2)^2$

- ⇒ Show that the maximum of this  $B(E1)$  distribution is located at  $E_c = \frac{3}{5} S_n$ .

## Advanced CDCC applications

## Extension to 3-body projectiles



To extend the CDCC formalism, one needs to evaluate the new coupling potentials:

$$V_{n;n'}(\mathbf{R}) = \int d\mathbf{r} \phi_n^*(\mathbf{x}, \mathbf{y}) \{ V_{nt}(\mathbf{r}_1) + V_{nt}(\mathbf{r}_2) + V_{at}(\mathbf{r}_3) \} \phi_{n'}(\mathbf{x}, \mathbf{y})$$

☞  $\phi_n(\mathbf{x}, \mathbf{y})$  three-body WFs for bound and continuum states: hyperspherical coordinates, Faddeev, etc (difficult to calculate!)



## Calculation of three-body states in the HH formalism

$$\Psi^{j\mu}(\rho, \Omega) = \rho^{-5/2} \sum_{\beta} \chi_{\beta}^j(\rho) \mathcal{Y}_{\beta}^{j\mu}(\Omega) \quad \beta \equiv \{K, l_x, l_y, l, S_x, J; I\}$$

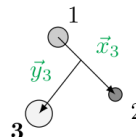
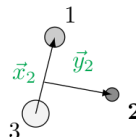
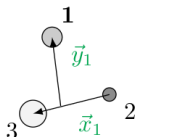
Hyperspherical Harmonics (HH) expansion

hypermomentum  $\hat{K}$

$$\mathcal{Y}_{\beta}^{j\mu}(\Omega) = \left[ \left( \Upsilon_{Klm_l}^{l_x l_y}(\Omega) \otimes \kappa_{S_x} \right)_J \otimes \phi_I \right]_{j\mu}$$

$$\Upsilon_{Klm_l}^{l_x l_y}(\Omega) = \varphi_K^{l_x l_y}(\alpha) [Y_{l_x}(\hat{x}) \otimes Y_{l_y}(\hat{y})]_{lm_l}$$

$$\varphi_K^{l_x l_y}(\alpha) = N_K^{l_x l_y} (\sin \alpha)^{l_x} (\cos \alpha)^{l_y} P_n^{l_x + \frac{1}{2}, l_y + \frac{1}{2}}(\cos 2\alpha)$$



**Jacobi  
coordinates**  
 $\{x, y, \hat{x}, \hat{y}\}$

**Hyperspherical  
coordinates**

$$\{\rho, \alpha, \hat{x}, \hat{y}\}$$

$$\rho = \sqrt{x^2 + y^2}$$

$$\alpha = \arctan \frac{x}{y}$$



## Calculation of three-body states in the HH formalism

$$\Psi^{j\mu}(\rho, \Omega) = \rho^{-5/2} \sum_{\beta} \chi_{\beta}^j(\rho) \mathcal{Y}_{\beta}^{j\mu}(\Omega) \quad \beta \equiv \{K, l_x, l_y, l, S_x, J; I\}$$

Hyperspherical Harmonics (HH) expansion

hypermomentum  $\hat{K}$

$$\mathcal{Y}_{\beta}^{j\mu}(\Omega) = \left[ \left( \Upsilon_{Klm_l}^{l_x l_y}(\Omega) \otimes \kappa_{S_x} \right)_J \otimes \phi_I \right]_{j\mu}$$

$$\Upsilon_{Klm_l}^{l_x l_y}(\Omega) = \varphi_K^{l_x l_y}(\alpha) [Y_{l_x}(\hat{x}) \otimes Y_{l_y}(\hat{y})]_{lm_l}$$

$$\varphi_K^{l_x l_y}(\alpha) = N_K^{l_x l_y} (\sin \alpha)^{l_x} (\cos \alpha)^{l_y} P_n^{l_x + \frac{1}{2}, l_y + \frac{1}{2}} (\cos 2\alpha)$$

Hyperradial functions are the solution of the coupled equations:

$$\left[ -\frac{\hbar^2}{2m} \left( \frac{d^2}{d\rho^2} - \frac{15/4 + K(K+4)}{\rho^2} \right) - \varepsilon \right] \chi_{\beta}^j(\rho) + \sum_{\beta'} V_{\beta' \beta}^{j\mu}(\rho) \chi_{\beta'}^j(\rho) = 0$$

with coupling potentials  $V_{\beta' \beta}^{j\mu}(\rho)$ . Model space defined by a given  $K_{max}$



## Calculation of three-body states in the HH formalism

$$V_{\beta'\beta}^{j\mu}(\rho) = \left\langle \mathcal{Y}_{\beta}^{j\mu}(\Omega) \middle| V_{12} + V_{13} + V_{23} \middle| \mathcal{Y}_{\beta'}^{j\mu}(\Omega) \right\rangle + \delta_{\beta\beta'} V_{3b}(\rho)$$

- $V_{ij}$  interaction between pairs  
central, spin-orbit, spin-spin, tensor. To reproduce binary subsystem
- $V_{3b}$  phenomenological three-body force  
diagonal term. Fixed to fine-tune the three-body energies

### Pseudo-State (PS) method

$$\chi_{\beta}^j(\rho) = \sum_{i=0}^N C_{i\beta}^j U_{i\beta}(\rho) \quad \text{expanded in } \mathcal{L}^2 \text{ basis}$$

$N$ : number of hyperradial excitations included

$$\mathcal{H}\Psi_n^{j\mu} = \varepsilon_n \Psi_n^{j\mu}$$

- $\varepsilon_n < 0$  **bound states**
- $\varepsilon_n > 0$  **discretized continuum**

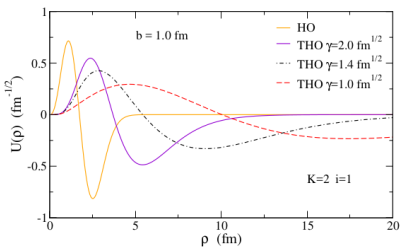


# Calculation of three-body states in the HH formalism

## Analytical Transformed Harmonic Oscillator (THO) basis

$$U_{i\beta}^{\text{THO}}(\rho) = \sqrt{\frac{ds}{d\rho}} U_{iK}^{\text{HO}}[s(\rho)]$$

$$s(\rho) = \frac{1}{\sqrt{2b}} \left[ \frac{1}{\left(\frac{1}{\rho}\right)^4 + \left(\frac{1}{\gamma\sqrt{\rho}}\right)^4} \right]^{\frac{1}{4}}$$

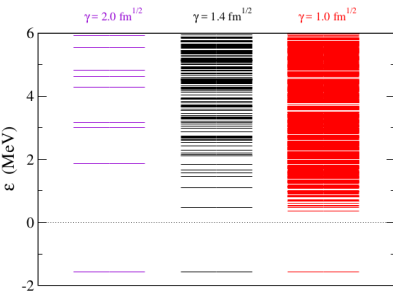


[PRC88(2013)014327]

## Example:

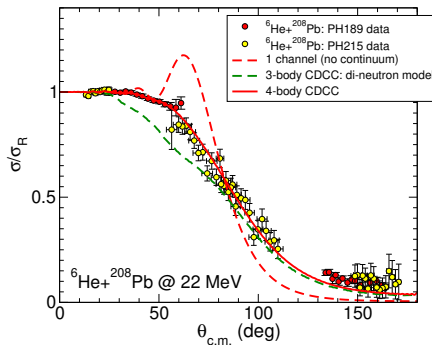
$\Psi_n^{j\mu}(\rho, \Omega)$  PS spectra,  $\varepsilon_n$   
 $b = 0.7 \text{ fm}$

The ratio  $\gamma/b$  controls the density of PS as a function of the energy.





## Four-body CDCC calculations for ${}^6\text{He}$ scattering



N.b.: 1-channel potential considers only g.s. → g.s. coupling potential:

$$V_{00}(\mathbf{R}) = \int d\mathbf{r} \phi_{\text{g.s.}}^*(\mathbf{x}, \mathbf{y}) \{ V_{nt}(\mathbf{r}_1) + V_{nt}(\mathbf{r}_2) + V_{ct}(\mathbf{r}_3) \} \phi_{\text{g.s.}}(\mathbf{x}, \mathbf{y})$$

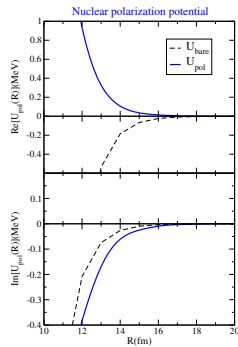
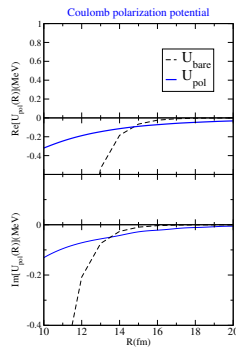
Data (LLN): Sánchez-Benítez et al, NPA 803, 30 (2008) L. Acosta et al, PRC 84, 044604 (2011)  
 Calculations: Rodríguez-Gallardo et al, PRC 80, 051601 (2009)



## Polarization potential from CDCC calculations

$$\left[ E - \varepsilon_0 - \hat{T}_{\mathbf{R}} - V_{0,0}(\mathbf{R}) \right] \chi_0(\mathbf{R}) = \sum_{i \neq 0} V_{i,0}(\mathbf{R}) \chi_i(\mathbf{R}) \equiv U_{\text{TELP}}(\mathbf{R}) \chi_0(\mathbf{R}).$$

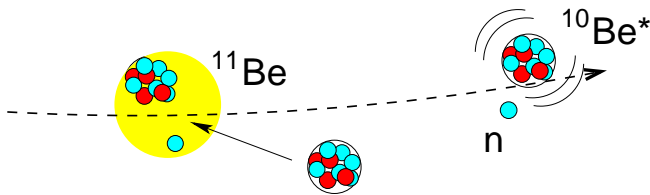
**Example:**  ${}^6\text{He} + {}^{208}\text{Pb}$  at 22 MeV



- ⇒ Polarization potentials are **long-ranged**.
- ⇒ Both **nuclear** and **Coulomb** couplings contribute to the polarization effect.

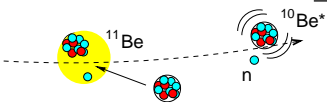
## Beyond the strict few-body picture: the effect of core excitation

To what extent can one ignore the dynamics of the core?



# Few-body versus Microscopic

## Microscopic models

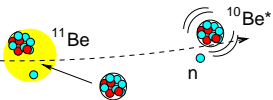


- ✓ Fragments described microscopically
- ✓ Realistic NN interactions (Pauli properly accounted for)
- ✗ Numerically demanding / not simple interpretation.



# Few-body versus Microscopic

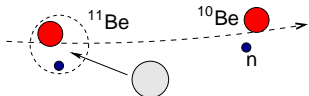
## Microscopic models



- ✓ Fragments described microscopically
- ✓ Realistic NN interactions (Pauli properly accounted for)
- ✗ Numerically demanding / not simple interpretation.

Many-body  
↑  
Few-body

## Inert cluster models

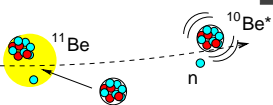


- ✗ Ignores cluster excitations (only few-body d.o.f.).
- ✗ Phenomenological inter-cluster interactions (aprox. Pauli).
- ✓ Exactly solvable (in some cases).
- ✓ Achieved for 3-body and 4-body (eg. coupled-channels, Faddeev).



# Few-body versus Microscopic

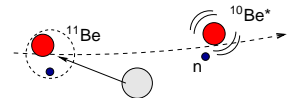
## Microscopic models



- ✓ Fragments described microscopically
- ✓ Realistic NN interactions (Pauli properly accounted for)
- ✗ Numerically demanding / not simple interpretation.

Many-body

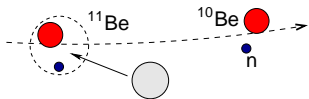
## Non-inert-core few-body models



- ✓ Few-body + some relevant collective d.o.f.
- ✓ Pauli approximately accounted for.
- ✓ Achieved for 3-body problems (coupled-channels, Faddeev).

Few-body

## Inert cluster models



- ✗ Ignores cluster excitations (only few-body d.o.f.).
- ✗ Phenomenological inter-cluster interactions (aprox. Pauli).
- ✓ Exactly solvable (in some cases).
- ✓ Achieved for 3-body and 4-body (eg. coupled-channels, Faddeev).



## Effect of core excitation in scattering observables

- ⇒ **Elastic** scattering (adiabatic recoil model): K. Horii *et al*, PRC81 (2010) 061602
  - ⇒ Some effects found in  ${}^8\text{B} + {}^{12}\text{C}$ .
- ⇒ Transfer (DWBA, CCBA, Faddeev): Winfield *et al*, NPA 683 (2001) 48, Fortier *et al*, PLB 461 (1999) 22, Deltuva, Phys.Rev. C 88, 011601 (2013)
- ⇒ Knock-out: Batham et al, PRC71, 064608 (2005)
  - ⇒ Small effect on stripping; large effect on diffraction
- ⇒ Breakup
  - DWBA: Crespo *et al*, PRC83, 044622 (2011), A.M.M. *et al* PRC85, 054613 (2012), A.M.M. and J.A. Lay, PRL109, 232502 (2012)
  - CDCC: Summers *et al*, PRC74, 014606(2006), PRC76,014611 (2007), De Diego *et al*, PRC89, 064609 (2014), PRC 95, 044611 (2017)

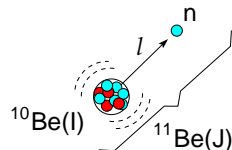


## How do core excitations affect the breakup of weakly-bound nuclei?

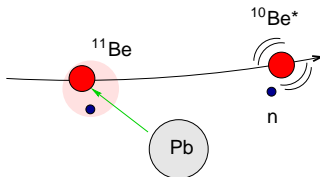
Core excitations will affect:

- ① the **structure** of the projectile  $\Rightarrow$  core-excited admixtures

$$\Psi_{JM}(\vec{r}, \xi) = \sum_{\ell,j,I} [\varphi_{\ell,j,I}^J(\vec{r}) \otimes \Phi_I(\xi)]_{JM}$$



- ② the **dynamics**  $\Rightarrow$  collective excitations of the  $^{10}\text{Be}$  during the collision compete with halo (single-particle) excitations.



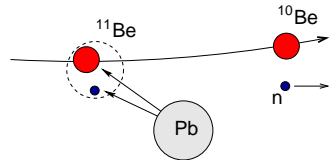
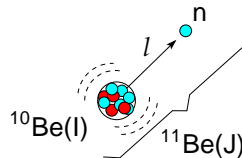
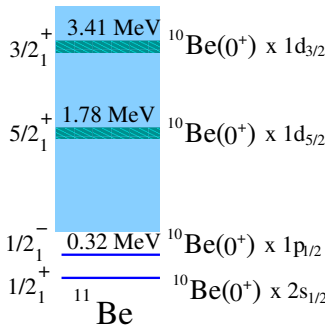
$\Rightarrow$  Both effects have been recently implemented in an extended version of the CDCC formalism (CDCC): Summers *et al*, PRC74 (2006) 014606, R. de Diego *et al*, PRC 89, 064609 (2014)



## Core excitation in reactions: *frozen-halo* picture

$$\Psi_{JM}(\vec{r}, \xi) = [\varphi_{\ell,j}^J(\vec{r}) \otimes \Phi_I(\xi)]_{JM}$$

- ⇒  $\varphi_{\ell,j}^J(\vec{r})$ = valence particle wavefunction
- ⇒  $\Phi_I(\xi)$ = core wavefunction (*frozen*)

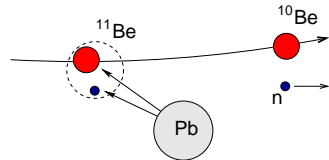
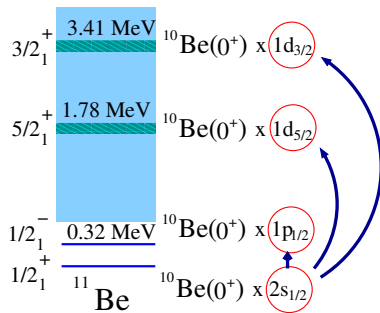
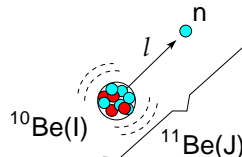




## Core excitation in reactions: *frozen-halo* picture

$$\Psi_{JM}(\vec{r}, \xi) = [\varphi_{\ell,j}^J(\vec{r}) \otimes \Phi_I(\xi)]_{JM}$$

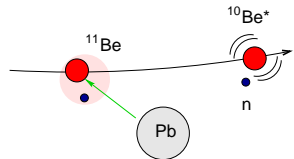
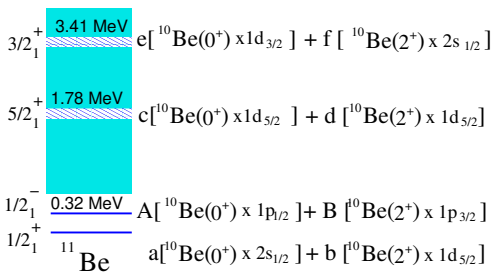
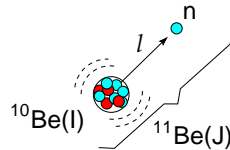
- ⇒  $\varphi_{\ell,j}^J(\vec{r})$  = valence particle wavefunction
- ⇒  $\Phi_I(\xi)$  = core wavefunction (*frozen*)





## Core excitation mechanism in breakup

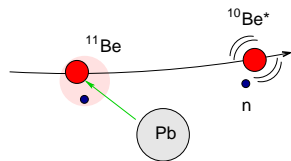
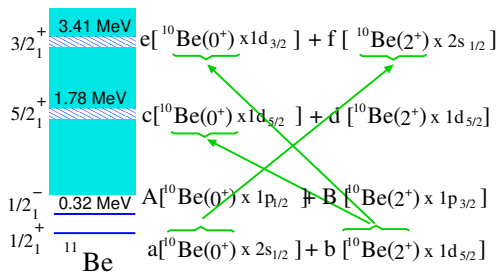
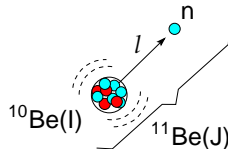
$$\Psi_{JM}(\vec{r}, \xi) = \sum_{\ell,j,I} [\varphi_{\ell,j,I}^J(\vec{r}) \otimes \Phi_I(\xi)]_{JM}$$





## Core excitation mechanism in breakup

$$\Psi_{JM}(\vec{r}, \xi) = \sum_{\ell,j,I} [\varphi_{\ell,j,I}^J(\vec{r}) \otimes \Phi_I(\xi)]_{JM}$$



☞ Dynamic core excitation contributes to the inelastic/breakup probabilities



## Extending CDCC to include core excitations

⇒ Standard CDCC ⇒ use coupling potentials:

$$V_{\alpha;\alpha'}(\mathbf{R}) = \langle \Psi_{J'M'}^{\alpha'}(\vec{r}) | V_{vt}(r_{vt}) + V_{ct}(r_{ct}) | \Psi_{JM}^{\alpha}(\vec{r}) \rangle$$

⇒ Extended CDCC (XCDCC) ⇒ use generalized coupling potentials

$$V_{\alpha;\alpha'}(\mathbf{R}) = \langle \Psi_{J'M'}^{\alpha'}(\vec{r}, \xi) | V_{vt}(r_{vt}) + V_{ct}(r_{ct}, \xi) | \Psi_{JM}^{\alpha}(\vec{r}, \xi) \rangle$$

- ☞  $\Psi_{JM}^{\alpha}(\vec{r}, \xi)$ : projectile WFs involving core-excited admixtures (**structure**).
- ☞  $V_{ct}(r_{ct}, \xi)$ : non-central potential allowing for core excitations/de-exitations (**dynamic** core excitation).

- Summers *et al.*, PRC74 (2006) 014606 (bins)
- R. de Diego *et al.*, PRC 89, 064609 (2014) (THO pseudo-states)

## Evidences of core excitation in nuclear breakup



## Structure part: particle-core model

- ⇒ Particle-plus-core Hamiltonian:

$$H_{\text{proj}} = T_r + h_{\text{core}}(\xi) + V_{vc}(\vec{r}, \xi)$$

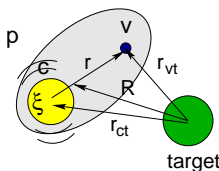
- ⇒ Projectile states expanded in  $|\alpha; JM\rangle \equiv |(\ell s)j, I; JM\rangle$  basis:

$$\Psi_{JM}(\vec{r}, \xi) = \sum_{\ell, j, I} R_{\ell, j, I}^J(r) \left[ [Y_\ell(\hat{r}) \otimes \chi_s]_j \otimes \Phi_I(\xi) \right]_{JM}$$

- ⇒ The unknowns  $R_{\ell, j, I}^J(r)$  can be obtained by direct integration of the Schrödinger equation or by diagonalization in a suitable discrete basis (pseudo-state method).



## Valence-core and core-target interactions in a simple collective model



⇒ Valence-core:

$$V_{vc}(\vec{r}, \xi) \simeq V_{vc}^{(0)}(r) - \delta_2 \frac{dV_{vc}^{(0)}}{dr} Y_{20}(\hat{r})$$

⇒ Core-target:

$$V_{ct}(\vec{r}_{ct}, \xi) \simeq \underbrace{V_{ct}^{(0)}(r_{ct})}_{\text{Valence excitation}} - \underbrace{\delta_2 \frac{dV_{ct}^{(0)}}{dr} Y_{20}(\hat{r}_{ct})}_{\text{Core excitation}}$$

$$\delta_2 = \beta_2 R_0 = \text{deformation length}$$

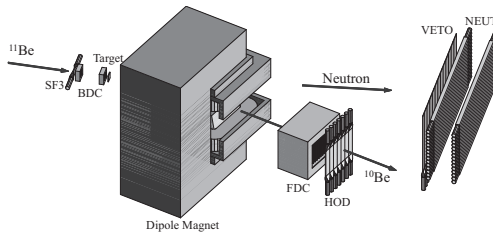
⇒ More sophisticated models for the projectile structure and core-target interaction are possible!



## Exclusive breakup measurements of halo nuclei

### RIKEN experiments:

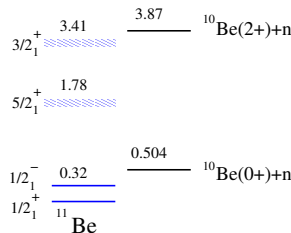
- ☞  $^{19}\text{C} + \text{p}$ : Satou et al., PLB660 (2008) 320
- ☞  $^{11}\text{Be} + ^{12}\text{C}$ : Fukuda et al, PRC70, 054606 (2004)



- ☞ Excitation energy and angular distribution of the projectile can be reconstructed from core-neutron coincidences (*invariant mass method*)



## Application to $^{11}\text{Be}$ : spectroscopic factors



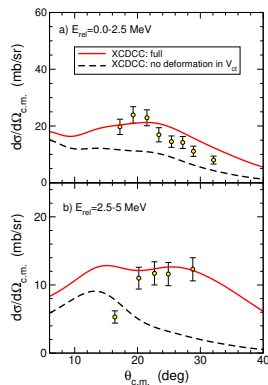
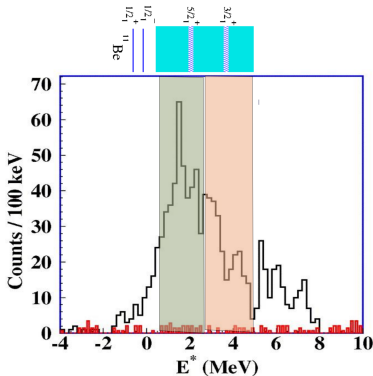
State	Model	$ 0^+ \otimes (\ell s)j\rangle$	$ 2^+ \otimes s_{1/2}\rangle$	$ 2^+ \otimes d_{5/2}\rangle$
$1/2_1^+$ (g.s.)	PRM	0.857	–	0.121
	SM (WBT)	0.76	–	0.184
$5/2_1^+$ (1.78 MeV)	PRM	0.702	0.177	0.112
	SM(WBT)	0.682	0.177	0.095
$3/2_1^+$ (3.41 MeV)	PRM	0.165	0.737	0.081
	SM(WBT)	0.068	0.534	0.167

- ⇒  $1/2_1^+, 5/2_1^+ \Rightarrow$  dominant  $^{10}\text{Be}(\text{gs}) \otimes nlj$  configuration
- ⇒  $3/2_1^+ \Rightarrow$  dominant  $^{10}\text{Be}(2^+) \otimes 2s_{1/2}$  configuration



## Evidence of *dynamical* core excitations in p( $^{11}\text{Be},\text{p}'$ ) at 64 MeV/u (MSU)

Data: Shrivastava et al, PLB596 (2004) 54 (MSU)



R.de Diego et al, PRC85, 054613 (2014)

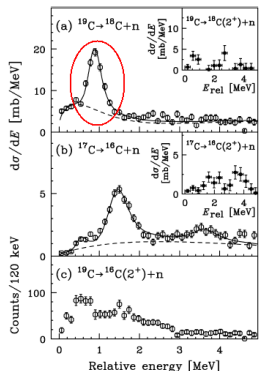
- ⇒  $E_{rel}=0\text{--}2.5$  MeV contains  $5/2^+$  resonance (expected **single-particle** mechanism)
- ⇒  $E_{rel}=2.5\text{--}5$  MeV contains  $3/2^+$  resonance (expected **core excitation** mechanism)

⇒ Dynamical core excitations give additional (and significant!) contributions to breakup

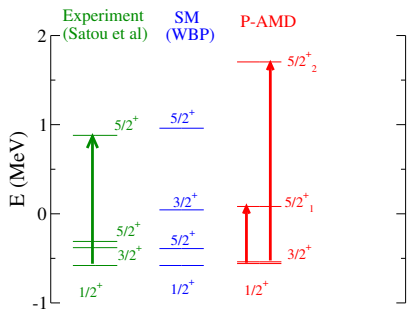


## Dominance of *dynamical* core excitations in $^{19}\text{C}$ resonant breakup

$^{19}\text{C} + \text{p} \rightarrow ^{18}\text{C} + \text{n} + \text{p}$  @ 70 MeV/u (RIKEN)



Satou et al, PLB660 (2008) 320

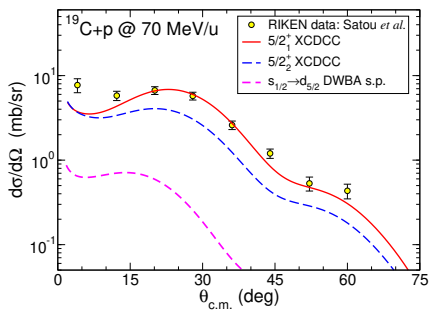
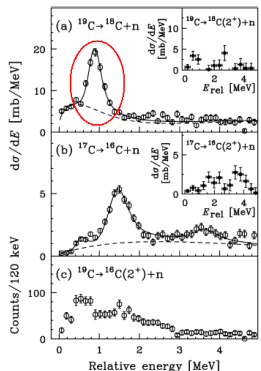


- ⇒ No general consensus about the  $^{19}\text{C}$  spectrum.
- ⇒ Resonant peak consistent with  $5/2_1^+$ ,  $5/2_2^+$  or even a combination of both.



# Dominance of dynamical core excitations in $^{19}\text{C}$ resonant breakup

$^{19}\text{C} + \text{p} \rightarrow ^{18}\text{C} + \text{n} + \text{p}$  @ 70 MeV/u (RIKEN)



J.A. Lay *et al.*, PRC 94, 021602 (2016)

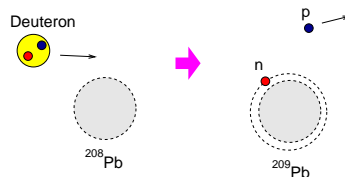
Satou *et al.*, PLB660 (2008) 320

⇒ The core-excitation mechanism gives the dominant contribution to the cross section

## Transfer reactions



## Outline



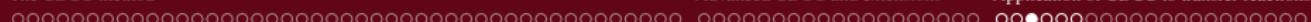
Example:  $d + ^{208}\text{Pb} \rightarrow p + ^{209}\text{Pb}$

### ① What do we measure in a transfer reaction?

- ① For a typical transfer reaction (e.g.  $d + ^{208}\text{Pb} \rightarrow p + ^{209}\text{Pb}$ ), one measures the **angular** and **energy** distribution of outgoing fragments (e.g. protons).
- ② Additionally, one may collect information of decay products of  $^{209}\text{Pb}$  (e.g.  $\gamma$ -rays,  $n$ ,  $p$ , etc)

### ② What information can we infer from a transfer reaction?

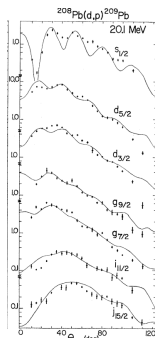
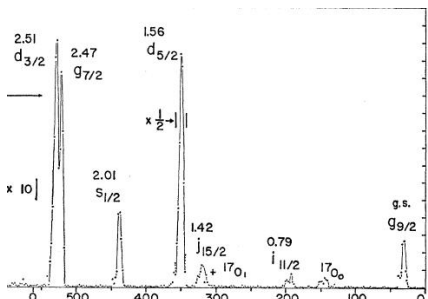
- ① **Excitation energies** of the residual nucleus ( $^{209}\text{Pb}$ ).
- ② **Angular momentum** assignment.
- ③ Single-particle content of populated states (i.e. **spectroscopic factors**).



## What do we measure in a transfer reaction?

Example:  $d + {}^{208}\text{Pb} \rightarrow p + {}^{209}\text{Pb}$

Phys. Rev. 159 (1967) 1039

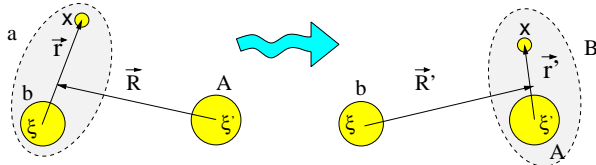


- ☞ The proton energy spectrum shows some peaks which reflect the **energy spectrum** of the residual nucleus ( ${}^{209}\text{Pb}$ ).
- ☞ Each peak has a characteristic **angular distribution**, which depends on the structure of the associated state.
- ☞ The population probability will depend on the **reaction dynamics** and on the **structure properties** of these states.

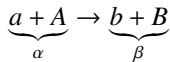


## DWBA method for transfer reactions

⇒ Transfer process:  $\underbrace{(b + x) + A}_{a} \rightarrow b + \underbrace{(A + x)}_{B}$

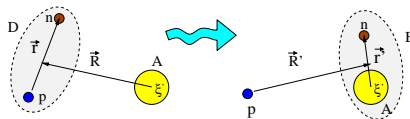


⇒ Complications arise with respect to inelastic scattering because now we have two different mass partitions involved





## The important ( $d, p$ ) case



- Introduce auxiliary potentials in entrance ( $U_\alpha(\mathbf{R})$ ) and exit ( $U_\beta(\mathbf{R}')$ ) channels.
- Projectile-target interaction:  $V_\beta = V_{pn} + U_{pA} = U_{pB}(\mathbf{R}') + \underbrace{V_{pn} + U_{pA} - U_{pB}}_{\Delta V_\beta} \equiv U_\beta(\mathbf{R}') + \Delta V_\beta$
- Post-form DWBA transition amplitude:

$$\mathcal{T}_{d,p}^{\text{DWBA}} = \int \int \underbrace{\chi_p^{(-)*}(\mathbf{K}_p, \mathbf{R}') \Phi_B(\xi', \mathbf{r}')}_{\text{Final state}} \underbrace{(V_{pn} + U_{pA} - U_{pB})}_{\Delta V_\beta} \underbrace{\chi_d^{(+)}(\mathbf{K}_d, \mathbf{R}) \varphi_d(\mathbf{r}) \phi_A(\xi') d\xi' d\mathbf{r}' d\mathbf{R}'}_{\text{Initial state}}$$

- ⇒  $\chi_{a,\beta}^{(\pm)}$  are distorted waves for entrance and exit channels, obtained with the optical potentials  $U_\alpha(\mathbf{R})$ ,  $U_\beta(\mathbf{R}')$
- For medium-mass/heavy targets:  $U_{pA} \approx U_{pB} \Rightarrow V_{pn} + U_{pA} - U_{pB} \approx V_{pn}(\mathbf{r})$



## $(d, p)$ case: parentage decomposition of target nucleus

⇒ Approximation of the **overlap integral**

$$\int d\xi' \phi_B^*(\xi', \mathbf{r}') \phi_A(\xi') \approx C_{BA}^{\ell j} \varphi_{nA}^{\ell j}(\mathbf{r}')$$

- $C_{BA}^{\ell j}$  = spectroscopic amplitude
- $|C_{BA}^{\ell j}|^2 = S_{BA}^{\ell j}$  = spectroscopic factor
- $\varphi_{nA}^{\ell j}(\mathbf{r}')$  = single-particle wavefunction describing motion of  $n$  with respect to  $A$ .

$$\mathcal{T}_{d,p}^{\text{DWBA}} = C_{BA}^{\ell j} \int \int \chi_p^{(-)*}(\mathbf{K}_p, \mathbf{R}') \varphi_{nA}^{\ell j,*}(\mathbf{r}') V_{pn}(\mathbf{r}) \chi_d^{(+)}(\mathbf{K}_d, \mathbf{R}) \varphi_d(\mathbf{r}) d\mathbf{r}' d\mathbf{R}'$$

$$\left( \frac{d\sigma}{d\Omega} \right)_{\beta,\alpha} = \frac{\mu_\alpha \mu_\beta}{(2\pi\hbar^2)^2} S_{BA}^{\ell j} \left| \int \int \chi_p^{(-)*}(\mathbf{K}_p, \mathbf{R}') \varphi_{nA}^{\ell j,*}(\mathbf{r}') V_{pn}(\mathbf{r}) \chi_d^{(+)}(\mathbf{K}_d, \mathbf{R}) \varphi_d(\mathbf{r}) d\mathbf{r}' d\mathbf{R}' \right|^2$$

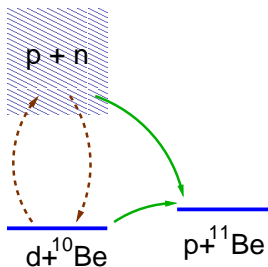
⇒ In DWBA, the  $(d, p)$  cross section is proportional to the spectroscopic factor. Comparing the data with DWBA calculations, one can extract the values of  $S_{BA}^{\ell j}$

## Application of CDCC to transfer reactions



## Transfer reactions with weakly bound nuclei

- ⇒ DWBA approximates the total WF by the elastic channel and assumes that the transfer occurs in one step (Born approximation).
- ⇒ For weakly bound projectiles (eg. deuterons), breakup is an important channel and can influence the transfer process.



- ⇒  $\Psi_{\mathbf{K}_d}^{(+)}(\mathbf{R}, \mathbf{r})$  includes breakup components, but these are lost when we make the DWBA approximation ( $\Psi^{(+)} \approx \chi_d^{(+)}(\mathbf{K}_d, \mathbf{R})\varphi_d(\mathbf{r})$ )  $\Rightarrow$  need to go beyond DWBA



## Adiabatic distorted wave approximation (ADWA)

- ⇒  $\chi_d^{(+)}(\mathbf{K}_d, \mathbf{R})$  describes deuteron elastic scattering but, for the  $(d, p)$  transfer matrix element, we need only  $\Psi_{\mathbf{K}_d}^{(+)}(\mathbf{R}, \mathbf{r})$  for small  $|\mathbf{r}|$
- ⇒ R.C. Johnson and col. have derived an approximation of  $\Psi_{\mathbf{K}_d}^{(+)}(\mathbf{R}, \mathbf{r})$  valid for  $r \approx 0$ , which includes the effect of deuteron breakup effectively (adiabatic approx.):

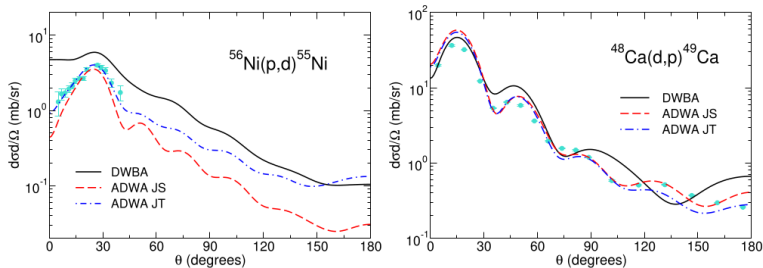
① Zero-range approximation (Johnson-Soper):

$$U^{JS}(R) = U_{pb}(R) + U_{nb}(R) \Rightarrow \chi_d^{JS}(\mathbf{R})$$

② Finite-range version (Johnson-Tandy):

$$U^{JT}(R) = \frac{\langle \varphi_{pn}(\mathbf{r}) | V_{pn} (U_{nb} + U_{pb}) | \varphi_{pn}(\mathbf{r}) \rangle}{\langle \phi_{pn}(\mathbf{r}) | V_{pn} | \phi_{pn}(\mathbf{r}) \rangle}$$

## DWBA vs ADWA



From Timofeyuk and, Progress in Particle and Nuclear Physics 111 (2020) 103738



## CDCC-BA approximation

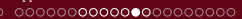
- Exact transition amplitude for a general  $\alpha \rightarrow \beta$  process:

$$\mathcal{T}_{d,p}^{\text{CDCC}} = C_{\text{BA}}^{\ell j} \int \int \chi_p^{(-)*}(\mathbf{K}_p, \mathbf{R}') \varphi_{nA}^{\ell j,*}(\mathbf{r}') V_{pn}(\mathbf{r}) \underbrace{\Psi_{\mathbf{K}_\alpha}^{(+)}(\mathbf{R}_\alpha, \xi_\alpha)}_{d\mathbf{r}' d\mathbf{R}'} d\mathbf{r}' d\mathbf{R}'$$

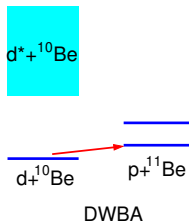
- Use CDCC approximation for  $\Psi_{\mathbf{K}_\alpha}^{(+)}$ :

$$\Psi_{\mathbf{K}_\alpha}^{(+)} \approx \Psi^{\text{CDCC}} = \underbrace{\chi_0(\mathbf{K}_\alpha, \mathbf{R}) \phi_0(\mathbf{r})}_{\text{elastic}} + \sum_{n', j, \pi} \underbrace{\phi_{n'}^{j\pi}(k_{n'}, \mathbf{r}) \chi_{n', j, \pi}(\mathbf{K}_{n'}, \mathbf{R})}_{\text{breakup}}$$

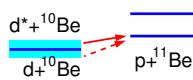
- Coupling to deuteron breakup states included explicitly.



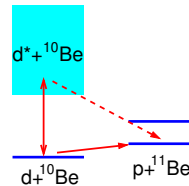
## DWBA, ADWA and CDCC-BA compared



DWBA



ADWA

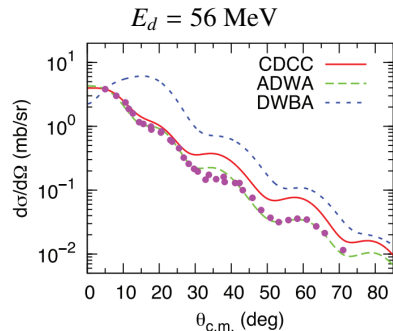
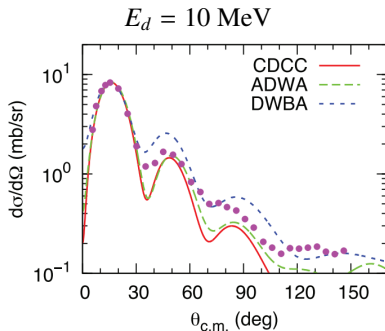


CDCC-BA



## DWBA vs ADWA vs CDCC

**Example:**  $^{58}\text{Ni}(\text{d},\text{p})^{59}\text{Ni}$



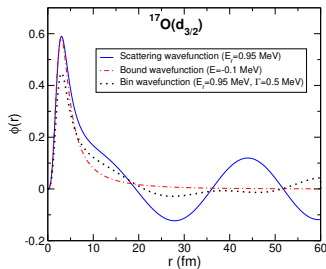
CDCC and ADWBA provide better description of the data and lead also to more realistic spectroscopic information (e.g. spectroscopic factors)

Pang *et al*, PRC 90, 044611 (2014)

## Exploring resonances from transfer reactions

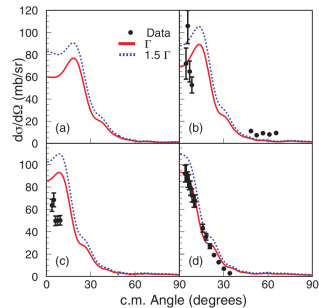
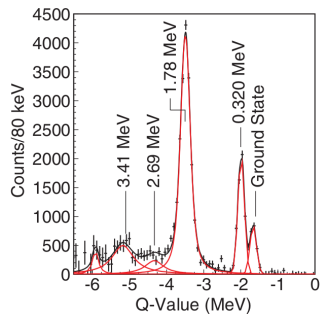
- ⇒ Inclusion of continuum states in DWBA poses numerical problems due to oscillatory behaviour of unbound wavefunctions
- ⇒ Some regularization method must be applied:
  - Representing the resonance by a weakly bound state with the same quantum numbers
  - Vincent & Fortune contour integration in the complex radius plane ([PRC2 \(1970\) 782](#))
  - Representing the resonance by a continuum *bin*

E.g.:  $d_{3/2}$  resonance in  $^{17}\text{O}$  resonance at  $E_r = 0.95 \text{ MeV}$





E.g.:  $^{11}\text{Be}$  resonance at  $E_x = 1.78 \text{ MeV}$  from  $^{10}\text{Be}(\text{d},\text{p})^{11}\text{Be}$

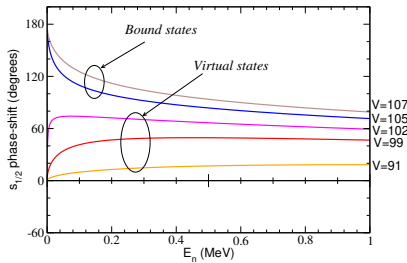


Schmitt et al, PRC88, 064612 (2013)

## Virtual states

- ⇒ Neutrons in *s*-wave cannot produce resonant states (no barrier)
- ⇒ Still, they can exhibit distinctive structures, characterized by a rapid increase of the phase-shift near zero energy (**virtual states**). This behaviour is commonly characterized in terms of the **scattering length**:

$$a_s = - \lim_{k \rightarrow 0} \tan \frac{\delta(k)}{k}$$



**Levinson theorem:**

$$\delta_\ell(E_n = 0) \rightarrow n\pi$$

( $n$ =number of bound states for partial wave  $\ell$ )

## Resonances and virtual states in the complex energy/momentum plane

- ⇒ A **bound state** is a normalizable solution of the Schrödinger equation for a imaginary momentum  $+i|k|$  and (negative) energy:  $E_s = \hbar^2(+i|k|)^2/2\mu = -\hbar^2|k|^2/2\mu$ .
- ⇒ A **virtual state** is a non-normalizable solution of the Schrödinger equation for a imaginary momentum  $-i|k|$  and (negative) energy:  $E_s = \hbar^2(-i|k|)^2/2\mu = -\hbar^2|k|^2/2\mu$ .

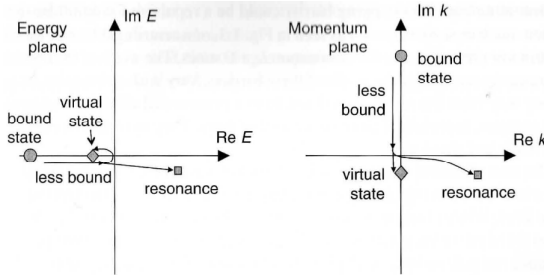
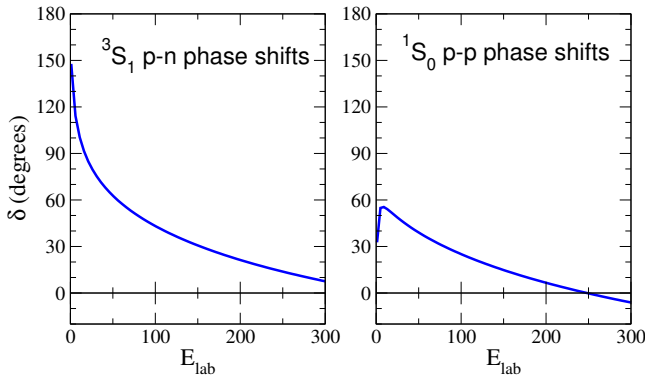


Fig. 3.4. The correspondences between the energy (left) and momentum (right) complex planes. The arrows show the trajectory of a bound state caused by a progressively weaker potential: it becomes a resonance for  $L > 0$  or when there is a Coulomb barrier, otherwise it becomes a virtual state. Because  $E \propto k^2$ , bound states on the positive imaginary  $k$  axis and virtual states on the negative imaginary axis both map onto the negative energy axis.

(figure borrowed from Thompson & Nunes' book)



## Bound vs virtual (anti-bound) states in the N-N system



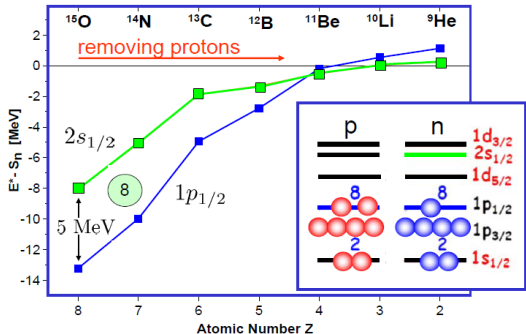
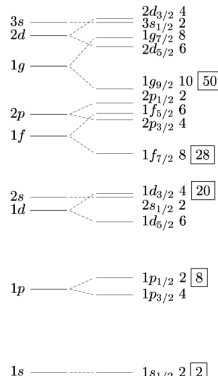
- ⇒  $p - n$ :  $\delta(E) \xrightarrow{E \rightarrow 0} \pi \Rightarrow$  one-bound state (deuteron)
- ⇒  $p - p, n - n$ : no bound states, but they do have an anti-bound (virtual) state.
- ⇒  $p - p$ :  $\delta$  becomes negative for large  $E \Rightarrow$  evidence of repulsive core!



# Spectroscopy in the continuum: shell evolution with neutron/proton asymmetry

⇒ Systematic studies of shell evolution requires extensions to the continuum

## Shell-evolution for N=7 isotones



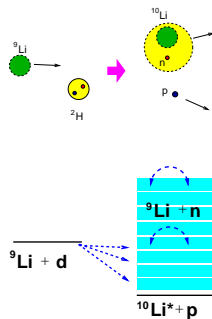
From: P.G. Hansen and J.A. Tostevin, Ann Rev Nucl Part Sci 53 (2003) 219

SM explanation: Otsuka et al, PRL95,232502(2005)

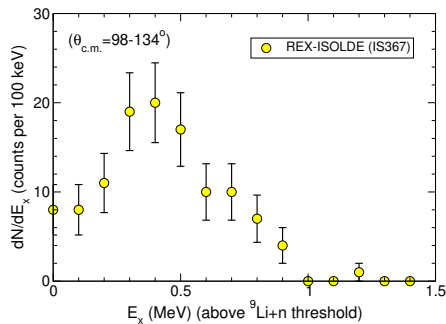


## Spectroscopy in the continuum: the ${}^{10}\text{Li}$ case

- Detected protons carry information on the  ${}^9\text{Li} + \text{n}$  excitation spectrum.

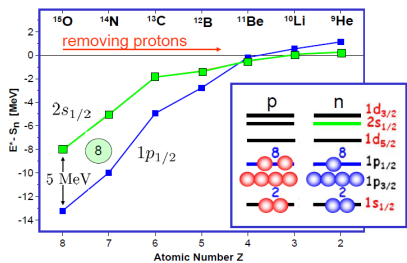


H.P. Jeppesen et al, PLB642 (2006) 449





# Populating resonances via transfer reactions ${}^9\text{Li}(\text{d},\text{p}){}^{10}\text{Li}^*$



From: P.G. Hansen and J.A. Tostevin, Ann Rev Nucl Part Sci 53 (2003) 219

HP. Jeppesen et al, PLB642 (2006) 449

